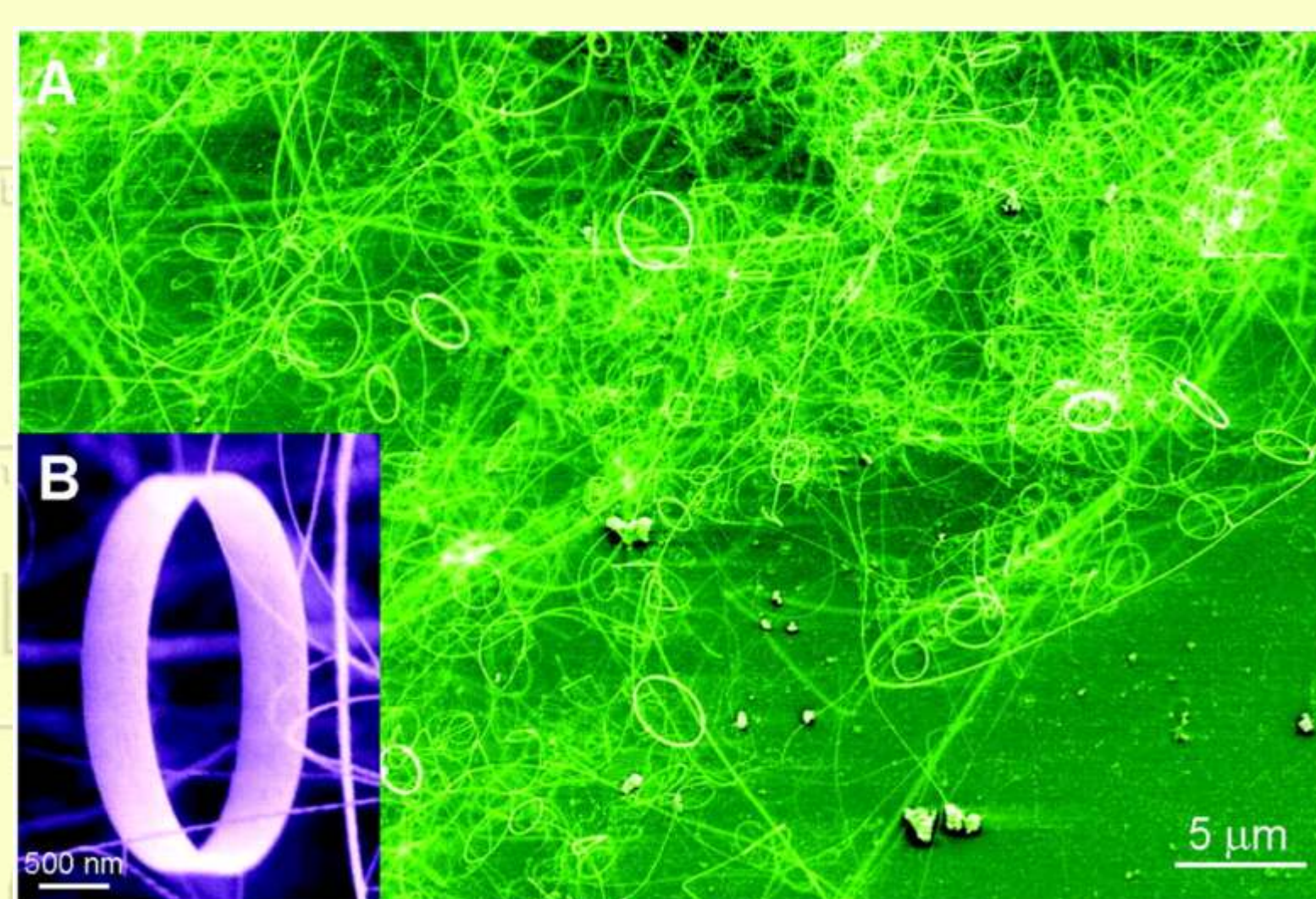


El senyor dels nanoanells

By coaxing a zinc oxide nanobelt—a long, thin ribbon composed of alternating layers of Zn^{2+} and O^{2-} , Zhong L. Wang and his coworkers at Georgia Institute of Technology have prepared the first freestanding, seamless, single-crystal nanorings out of ZnO [*Science*, **303**, 1348 (2004)]. These structures could be used to make semiconducting and piezoelectric-based nanoscale components that are biocompatible.

Since submitting the paper, the group has been able to fine-tune the process to produce more uniform rings. And now they are also able to manipulate individual nanorings.

The rings form when ZnO nanobelts spontaneously coil up. Over time, the coil's loops, which may be as few as five or as many as 100, become sintered together into a single crystal.



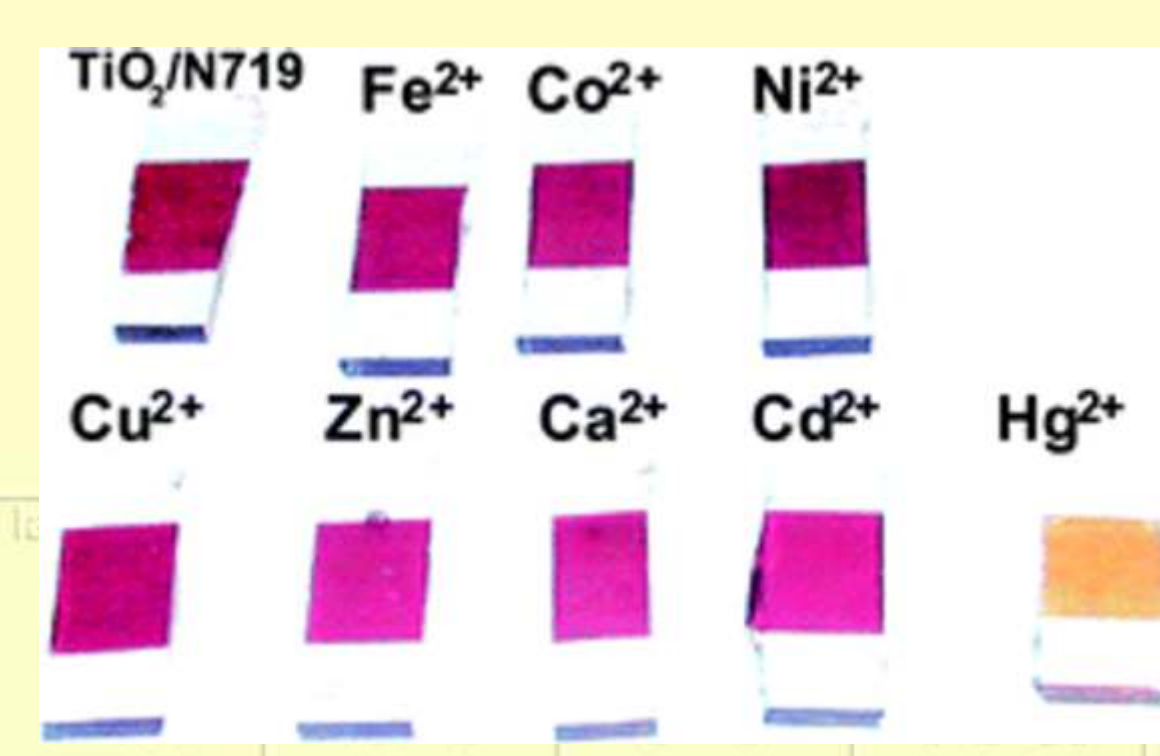
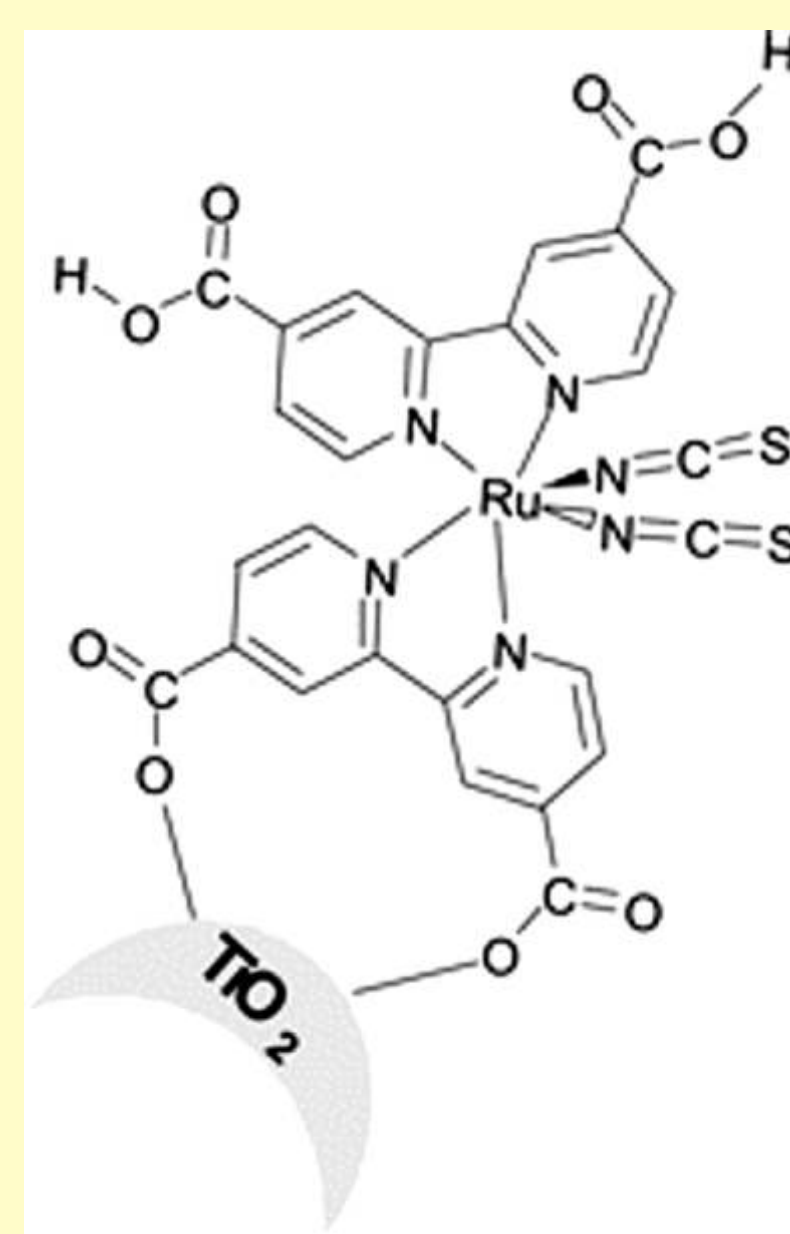
(A) Low-magnification SEM image of the as-synthesized ZnO nanorings. (B) High-magnification SEM image of a freestanding single-crystal ZnO nanoring, showing uniform and perfect geometrical shape. The ring diameter is 1 to 4 μm , the thickness of the ring is 10 to 30 nm, and the width of the ring shell is 0.2 to 1 μm .

Detecció fàcil de mercuri(II)

A novel chemical sensor for the colorimetric detection of toxic mercuric salts in water exhibits submicromolar sensitivity, according to the chemists in the U.K. who designed the system [E. Palomares et al., *Chem. Commun.*, **2004**, 362].

The sensor is based on a mesoporous nanocrystalline TiO_2 film sensitized with a commercially available ruthenium dye. The film's color changes from red to orange when it is immersed in an aqueous solution of a Hg^{2+} salt.

Using the dye-sensitized film, the researchers can detect Hg^{2+} concentrations as low as 20 μM with the naked eye. Spectrophotometric detection using the film enabled them to sense Hg^{2+} concentrations down to around 0.3 μM —that is, 0.5 ppm of Hg^{2+} .

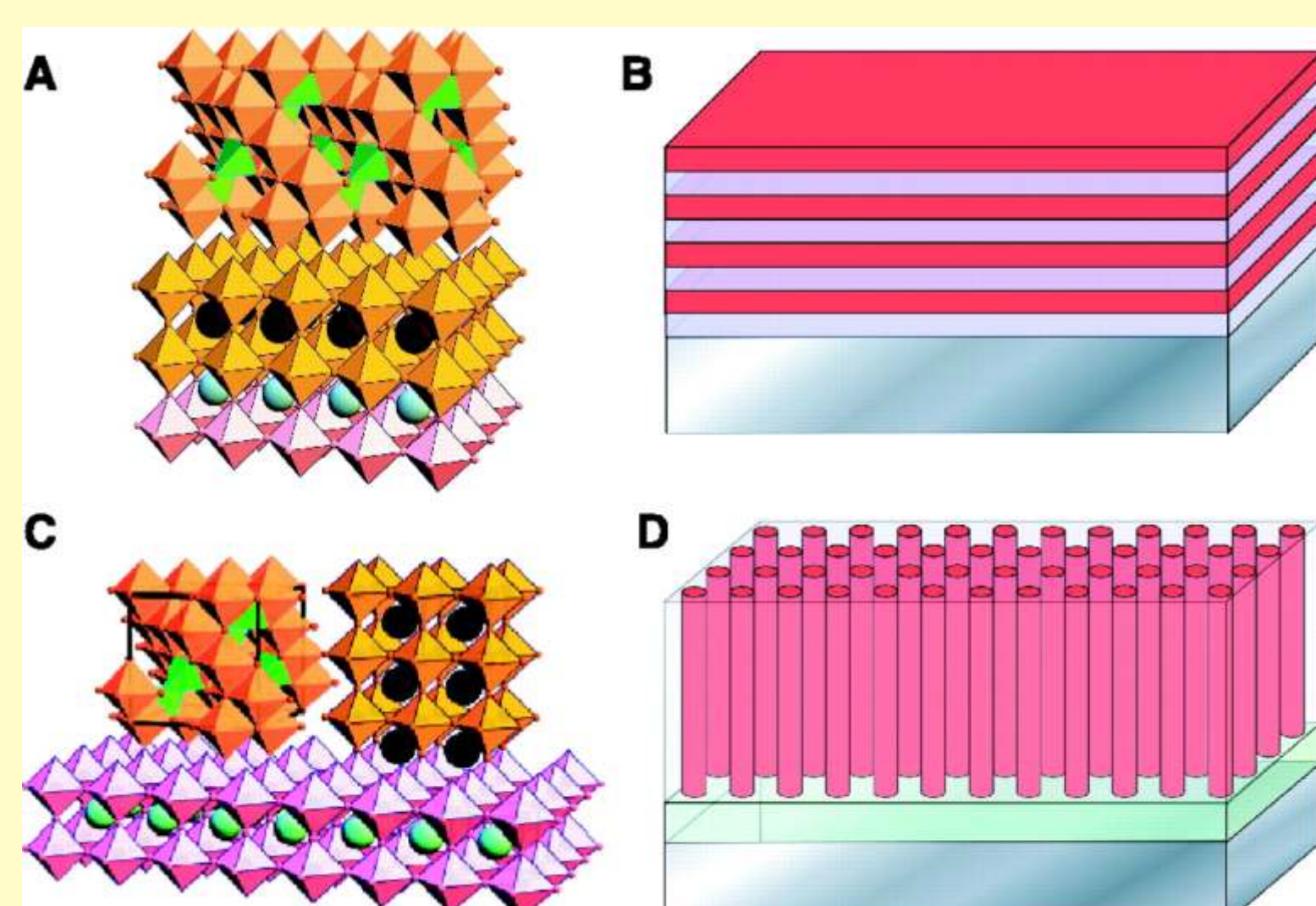


Materials multiferroics

A nanostructured multiferroic material with both ferroelectric and ferromagnetic properties is reported [H. Zheng et al., *Science*, **303**, 661 (2004)].

Using a self-assembly process ferromagnetic $CoFe_2O_4$ nanoparticles form pillars inside a ferroelectric $BaTiO_3$ ferroelectric matrix resulting in the multiferroic material.

The nanostructures were deposited on single-crystal $SrTiO_3$ substrates by pulsed laser deposition from a single Ba-Ti-Co-Fe-oxide target.



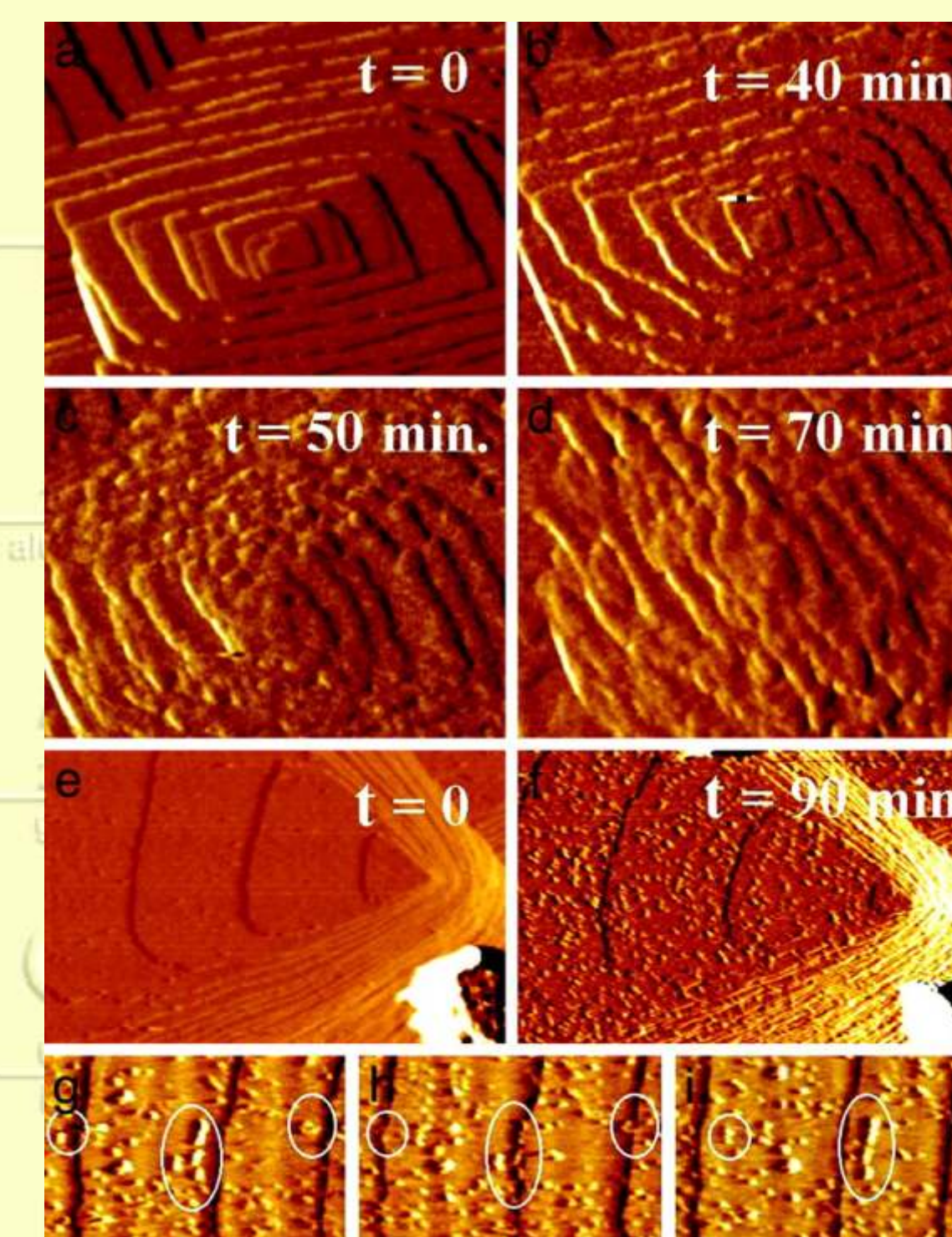
(A) Superlattice of a spinel (top) and a perovskite (middle) on a perovskite substrate (bottom). (B) Schematic illustration of a multilayer structure on a substrate. (C) Epitaxial alignment of a spinel (top left) and a perovskite (top right) on a perovskite substrate (bottom). (D) Schematic illustration of a self-assembled nanostructured thin film formed on the substrate.

Les pedres del ronyó, sota control

The molecular-scale mechanism by which two urinary constituents inhibit the growth of the major inorganic component of kidney stones has been studied [S.R. Qiu et al., *Proc. Natl. Acad. Sci.*, **101**, 1811 (2004)].

In-situ atomic force microscopy and molecular modelling were used to probe the inhibitory effects of citrate and osteopontin (OPN) on the crystallisation of calcium oxalate monohydrate (COM)—a major constituent of kidney stones.

Results indicate that the citrate modifies the shape and inhibits the growth of COM as a consequence of step-specific pinning on the (-101) face. Osteopontin, however, strongly inhibits the (010) face but has little effect on the (-101) face.



AFM images showing the effect of OPN on COM growth hillock morphology. (a–d) Sequential images (horizontal dimension, 1.7 μm) showing OPN modification of the growth hillocks on the (010) face by 5 nM OPN. (e and f) Sequential images (horizontal dimension, 6.0 and 4.5 μm) showing the effect of OPN on growth hillocks morphology of the (-101) face. (g–i) Temporal evolution of step train and protein adsorbates on the (-101) face (horizontal dimension, 2 μm).

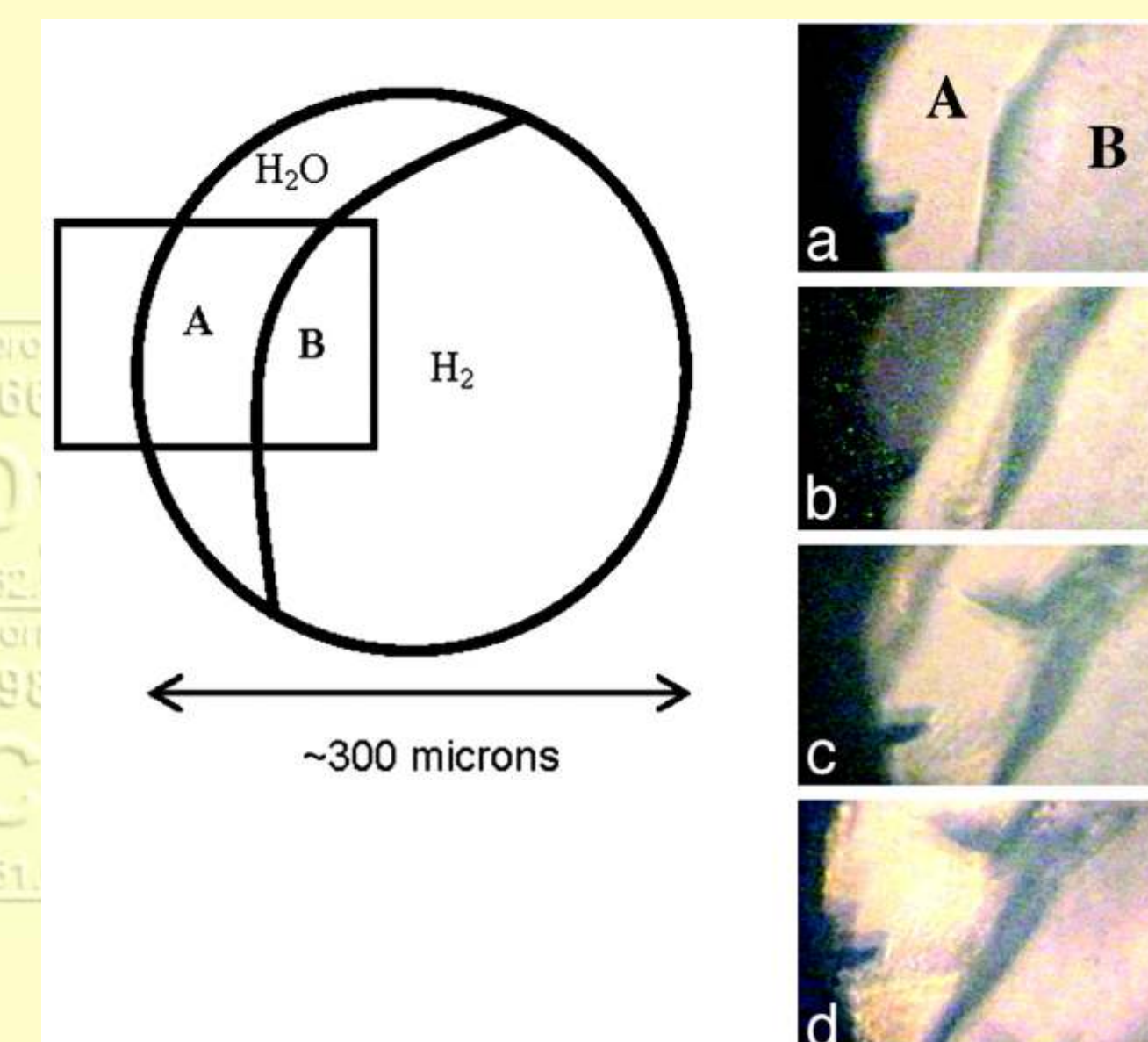
L'aigua, magatzem d'hidrogen

The hydrogen clathrate hydrate, $H_2(H_2O)_n$, was synthesized at 200–300 MPa and 240–249 K [W.L. Mao et al., *Proc. Natl. Acad. Sci.*, **101**, 708 (2004)].

Twelve experiments were carried out on three hydrogen–ice systems (9 hydrogen–water, 2 hydrogen–methane and 1 hydrogen–octane) in a diamond anvil cell (DAC). The DAC was introduced into a cryostat after filling with compressed hydrogen gas.

The systems were studied in situ by Raman and infrared spectroscopies, neutron diffraction and optical microscopy. The clathrate was held at ambient pressure at 77 K and hydrogen was subsequently released by heating to 140 K.

The ability of the hydrogen hydrate to hold 5.2 wt% hydrogen is in line with a US Department of Energy target of 4.5% by 2005.



Photomicrographs of hydrogen and water in the circular gasket hole at 300 MPa as viewed through the diamond windows. (a) At 250 K before the formation of clathrate, the crescent-shaped water in region A was clearly separated from the hydrogen in region B. (b) Cooling down to 249 K, a reaction zone of clathrate formed between hydrogen and water. The residual water darkened as clathrate nucleated. (c) The clathrate further grew at the expense of the water and hydrogen. (d) The reaction was completed after 30 min at 249 K. At this point, all of the water had transformed completely into clathrate.

Breus

• S'ha proposat un mètode alternatiu de preparació de silici més sostenible sense formació de CO_2 [*Angew. Chem. Int. Ed.*, **43**, 733 (2004)].

• Finalment, s'ha completat la sèrie de compostos $[MX_2(PR_3)_2]$ ($M=Pd, Pt$) amb la preparació dels fluoroderivats ($X=F$) [A. Yahav et al., *J. Am. Chem. Soc.*, **125**, 13634 (2003)].

• Una pàgina web amb la Taula Periòdica dels còmics: <http://www.uky.edu/Projects/Chemcomics>

L'element número 15, fòsfor, va ser descobert l'any 1669 per Henning Brand. El seu nom prové de la paraula grega *phos*, que vol dir *portador de la llum*.